



## ANALYSIS OF DENTAL ALLOYS CHARACTERISTICS (MICROSTRUCTURE AND CORROSION RESISTANCE) FOR DIFFERENT OBTAINING METHODS

**Ionuț ȘTIRBU, Petrică VIZUREANU, Nicanor CIMPOEȘU**

Technical University "Gh. Asachi" Iași  
e-mail: nicanornick@yahoo.com

### ABSTRACT

*A dental alloy was studied by electro-chemical polarization method, scanning electrons microscopy (S.E.M.) and X-ray dispersive energy analysis (EDAX) equipments analyzing the influence of casting process on microstructure and corrosion behaviour. These studies present that in natural aerated Afnor solution saliva this alloy behaves as a corrosion resistant alloy. By casting, this alloy undergoes a significant modifications of both internal microstructure and corrosion resistance. Using over-potentials bigger than five hundred mV (SCE) in artificial saliva this alloy exhibits a generalized corrosion, the surface morphology being dissimilar for commercial and as-cast samples. EDAX studies point out that corrosion takes place especially by cobalt dissolution.*

**KEYWORDS:** dental alloy, Co-Cr-Mo, potentiometry, EDX analysis, surface morphology

### 1. Introduction

The base-metal alloys have received recently considerable attention in biomedical field, because such alloys provide excellent strength, toughness and wear resistance. Cobalt-Chromium alloys are well used for biomedical applications such as fixed and removable partial denture framework and orthopaedic implants owing to their excellent mechanical properties, wear resistance and biocompatibility /1, 2/. Besides the economic advantage over gold, owing to their low cost, these alloys are attractive because they are less than half the density and are considerably stronger than gold. Co-Cr dental alloys have an excellent corrosion resistance, which is provided by a thin adherent layer of chromium-based oxides on the surface /3, 4/. The most used Cobalt base alloys for dentistry is Co-Cr-Mo with carbon content about 0.5 percent. Chromium and Molybdenum are substantial elements while Carbon is well known as interstitial element. It was stated that corrosion resistance of metallic denture prostheses depends on many factors, among other things on the chemical composition, surface structure and microstructure. Many of microstructure aspects such as: elements segregation and cast homogeneity, shrinkage and pores, sizes of grain boundaries or precipitates are directly subjected to the production engineering and manufacture of casts /5, 6/.

Venugopalan and Gaydon /7/, in a review of the corrosion behaviour of surgical implant alloys, observe that cobalt alloys do not show the traditional active-passive transition as they were also in a passive state prior to testing. The wrought and cast alloys do not exhibit a hysteresis loop in a potentiodynamic polarization curve, indicating that they can repair damage to their oxide/passive layer faster/better. The casting of these alloys is easily performed by the use of a gas-oxygen flame with a blowtorch. Nevertheless, the gas-air combustion in the blowtorch exposes the worked alloy to oxidation through the inclusion of carbon which might change the physical and corrosion properties of the alloy /8, 9/.

The aim of this study is to evaluate the influence of the casting process on the microstructure and the corrosion behaviour of a Co-Cr dental alloy

### 2. Experimental part

For these studies a "CH" trade mark dental alloy, produced and purchased by VASKUT Kohaszati Kft - Hungary, was used. This is a Co-Cr type dental alloy for prosthesis, crown, bridges and round bridges, having the composition:

Co = 62%, Cr = 30%, Mo = 5%, Si = 1%, C = 0.5%,  
Mn = 0.5%, W = 0.5%



The manufacturer indicates that the Co-Cr-Mo base alloys are suitable for producing corrosion resistant long life metal frameworks and plate casting, easy to process and polish providing an aesthetic outlook. The material meets ISO 6871-1, ISO TR 7405 and 93/42/EEC Council Directive prescriptions. From this commercial material a casting sample was obtained by melting in butane/oxygen flame and manual horizontal centrifugal machine, in a non-controlled casting environment.

Corrosion behavior was realized by rapid electrochemical tests, particularly by dynamic potentiometry. The measurements of open potential circuit and potentiodynamic polarizations were performed on a VoltaLab 21 Electrochemical System (PGP201 - Radiometer Copenhagen) equipped with the acquisition and processing data software VoltaMaster 4. A three-electrode electrochemical cell was used. From commercial and as-cast materials, the working electrodes were performed in cylindrical form and mounted in a Teflon support to enable the connection to rotating port-electrode of the electrochemical cell.

The free area was precisely measured before embedding in the Teflon support. A saturated calomel electrode (SCE) was used as a reference and platinum as auxiliary electrode.

Each specimen was polished with SiC paper, gradually, down up to 4000 grit specification, degreased with acetone and washed in distilled water.

As corrosion medium an aerated solution of Afnor artificial saliva (Carter-Brugirard AFNOR/NF (French Association of Normalization) 591-141) was used, having the composition: NaCl – 0.7 g/l, KCl – 1.2 g/l, Na<sub>2</sub>HPO<sub>4</sub>H<sub>2</sub>O – 0.26 g/l, NaHCO<sub>3</sub> – 1.5 g/l, KSCN – 0.33 g/l, urea – 1.35 g/l, and pH = 8.

Linear polarization measurements were performed, in aerated solution, at potentials near the  $E_{corr}$ , in the potential range  $\pm 150$  mV against the open circuit potential and a potential scan rate of 0.5 mV/s. The polarization resistance ( $R_p$ ) was calculated as tangent slope at the electrode potential vs. current density curve in the  $E_{corr}$  point. The cathodic Tafel slope ( $b_c$ ) was calculated as the potential change over one decade (one order of magnitude) decrease in the current density at potentials near the  $E_{corr}$ . The anodic Tafel slope ( $b_a$ ) was determined in a similar way.

Linear polarization method is used to determine when a test electrode is at its steady state. Polarization resistance is used to estimate the general corrosion rate of the metal.

On the basis of these data, the corrosion current density ( $J_{corr}$ ) - which is a measure of the corrosion rate, was calculated with the Stern-Geary equation:

$$J_{corr} = \frac{b_a b_c}{2.3 R_p (b_a + b_c)} \quad (1)$$

The corrosion rate, expressed as penetration rate - the layer thickness of the metal removed from the alloy surface in the time unity, was evaluated with the relation:

$$v_p = 3,27 \left( \frac{A}{z} \right) \frac{J_{corr}}{\rho}, \text{ } \mu\text{m/year} \quad (2)$$

where: A – is the atomic mass of the corrodible metal (g/mol), z – number of electrons changed in the corrosion process,  $\rho$  - density of the removed component (g/cm<sup>3</sup>) and  $J_{corr}$  – instantaneous current density ( $\mu\text{A}/\text{cm}^2$ ).

Three additional corrosion parameters: corrosion potential in dynamic conditions ( $E_{cor}$ ), breakdown potential ( $E_{BD}$ ) and re-passivation potential ( $E_{RP}$ ), were determined from the cyclic potentiodynamic polarization curve, performed at a potential scan rate of 10 mV/s, on the electrode potential range: -1500 to +1500 mV:

To evaluate the influence of the casting on the corrosion process and the surface morphology, an electrochemical treatment, consisting in five successive cyclic polarizations, was performed in 0...+1500 mV potential range, with a 10 mV/potential scan rate. First cycle was beginning on -1500 mV, view to electrochemical cleaning of the surface.

To study the microstructure of the two alloys samples their surface was chemically treated in agreement with standard procedures /10/. The treated surface was examined with using a XJP-6A type metallurgical microscope (China). After the electrochemical treatments, a study of the modifications of the alloys surface was performed on a VEGA-TESCAN Scanning Electron Microscope equipped with QUANTAX Bruker AXS Microanalysis system.

### 3. Results and discussions

The microstructures obtained for the two studied sample are shown in Figure 1.

For the wrought sample one can identify large amounts of precipitate along the interdendritic regions. Considering the ternary phase diagram of Co-Cr-Mo alloy, the precipitate in this high chromium alloy can be a mixture of Mo-concentrate R ( $\text{Co}_{49}\text{Cr}_{21}\text{Mo}_{30}$ ) and  $\mu(\text{Co}_7\text{Mo}_6)$  phase, or, more probable, chromium carbides like  $\text{Cr}_7\text{C}_3$  or  $\text{Cr}_{23}\text{C}_6$  due to presence of the C in alloy composition. The image for as-cast sample reveals a quite different aspect, a relatively ordered broken dendrite structure with large interdendritic zones. Using the QUANTAX Bruker AXS Microanalysis (GmbH, Berlin, Germany) the compositions of the commercial and casting „C” alloy, both before and after

electrochemical treatment, were evaluated. The obtained values are presented in Table 1.

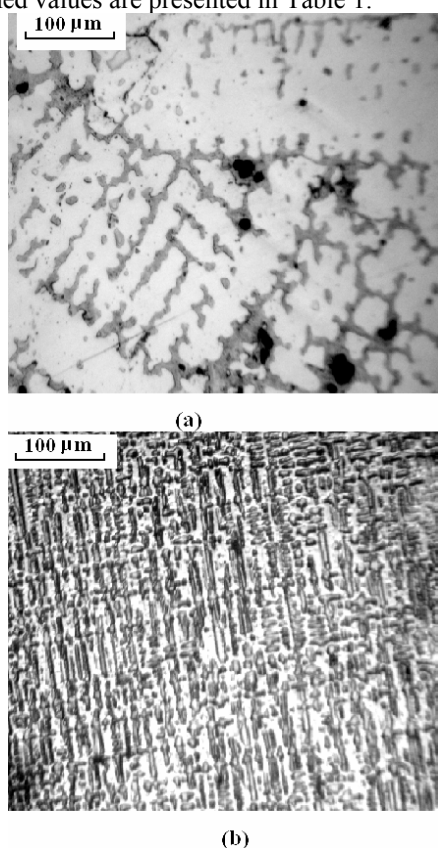


**Fig. 1.** Optical micrographs of commercial Co-Cr sample (a) and as-cast sample (b)

The composition of the commercial sample differs slightly comparing to the one indicated by manufacturer, the quantity of Cobalt being approximately 3% higher while the quantity of Chromium is more than 3% smaller. The performed microanalysis did not evidence the presence of Manganese (Mn) and Tungsten (W).

By casting, the alloy loses out more than 2% of Chromium, while the percentages of Mo, Si and C practically remain unchanged. The loss of Chromium percentage is reflected in a corresponding increase of the Cobalt percentage.

The five cycles of polarization in Afnor saliva lead to a superficial corrosion which produces a modification of the superficial composition of the alloy. This modification consists in a pronounced decrease of the Cobalt; about 24% for the commercial sample and 19% for the casting sample. This denotes that the corrosion process takes place by anodic dissolution of the Cobalt from the alloy.

More unlike the non-electrochemically treated sample, the microanalysis indicates that on both commercial and casting electrochemically treated surfaces a quantity of almost 12% Oxygen is present on alloy surface. This is probable due to formation of Cr<sub>2</sub>O<sub>3</sub> and MoO<sub>3</sub> oxides, which assure the higher resistances to corrosion at over-potentials lower than 700 mV (SCE).

The linear polarization curves, in semi-logarithmic coordinates (Evans diagram), and the cyclic polarization curves for the two studied samples are presented comparatively in figure 2.

**Table 1.** Superficial compositions of „CH” alloy, no processed and as cast, before and after electrochemical treatment in artificial Afnor saliva

Surface state	Sample	Element (wt %)					
		Co	Cr	Mo	Si	C	O
Non-corroded	Commercial alloy	65	26	6.0	0.5	1.5	-
	Casting alloy	67	24	6.0	0.5	1.3	-
Electrochemically processed	Commercial alloy	50	27	7.3	0.7	2.0	12
	Casting alloy	54	24	7.0	0.6	1.5	12.

From Evans diagram the corrosion parameters corresponding to the equilibrium state were evaluated. Corrosion potential ( $E_0 = E(I=0)$ ) - namely the potential where the total corrosion current is zero) and, Tafel constants ( $b_a$  and  $b_c$ ), polarization resistance ( $R_p$ ), instantaneous corrosion current density ( $J_{cor}$ ) and corrosion rate ( $v_{cor}$ ). From cyclic polarization curves the corrosion potential ( $E_{cor}$ ), breakdown potential ( $E_{BD}$ ) and re-passivation potential ( $E_{RP}$ ) were evaluated. Table 2 collates these parameters.

The corrosion potential in quasi equilibrium conditions (obtained at lower potential scan rate),  $E_0$ ,

is more negative for commercial sample than for the as-cast sample, this indicating a higher tendency of corrosion when the alloy is immersed in Afnor saliva. This is only an apparent situation because of the polarization resistance of commercial alloy in this artificial saliva is five time higher than that of the casting alloy. Accordingly, the instantaneous current density and corrosion rate are lower in the case of the wrought alloy. However, the differences regarding the corrosion behaviour of the two samples in Afnor saliva are not relevant. More, the values of the corrosion rates are very small, indicating a high corrosion resistance of this alloy.

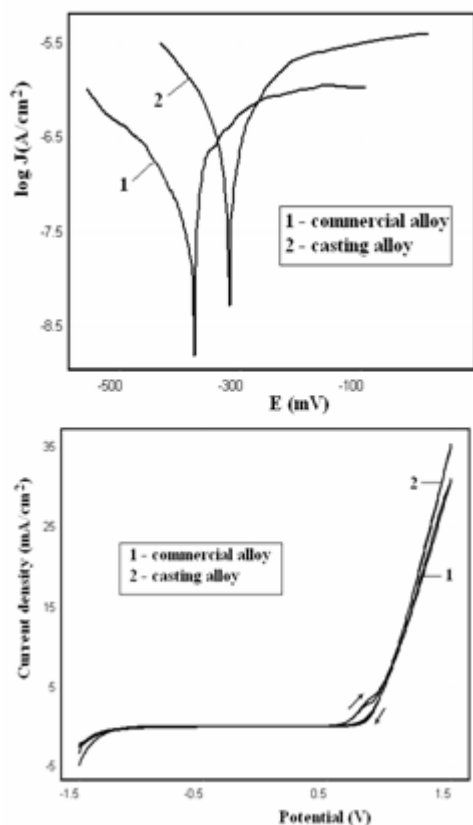


**Fig. 2.** Linear potentiodynamic polarization curve (a) and single cyclic polarization curve (b) for commercial (curve 1) and as-cast (curve 2) alloys

The cyclic voltammograms of the two sample showed a very close similarity (Fig. 2(b)); the two curves practically overlap. The two recorded curves revealed the passive region over a large domain of potential, from negative value to the breakdown potential situated at 557 and 523 mV (SCE) respectively. At over-potentials higher than the breakdown potential the corrosion currents increase appreciably and vary linearly with electrode over-potential, indicating a direct dependence between corrosion current and over-potential. The anodic and cathodic branches of the polarization curve in this domain practically overlap, excepting the potential range between  $E_{BD}$  and  $E_{RP}$ , where a small hysteresis loop appears. The slopes of the linear portions are 47.6 mA/(cm<sup>2</sup>.V) for the non-casting sample and 54.7 mA/(cm<sup>2</sup>.V) for the casting sample.

The current densities at 1500 mV potential electrode were 30.9 mA/cm<sup>2</sup> and 35.4 mA/cm<sup>2</sup> these values indicating higher corrosion rates of the alloy.

**Table. 2** Corrosion parameters evaluated from linear and cyclic polarization curves

Sample	Linear polarization					Cyclic polarization	
	$E_0$ , mV	$b_a$ , mV	$b_c$ , mV	$R_p$ , k $\Omega$ .cm <sup>2</sup>	$J_{cor}$ , $\mu$ A/cm <sup>2</sup>	$V_{cor}$ , $\mu$ m/an	$E_{RP}$ , mV
Commercial	-383	244	-441	366.7	0.262	3.07	452
As-cast	-318	136	-121	68.7	0.378	4.42	343

The voltammogram shapes indicate rather a general corrosion not a pitting corrosion.

This assertion is confirmed by Scanning Electron Microscopy (SEM) studies. Figure 3 shows SEM micrographs of the "C" alloy after the five cycle electrochemical treatment.

Figure 3 illustrates the generalized corrosion taking place as a result of the electrochemical treatment performed.

The surface morphology is very dissimilar for the two samples. In the case of the commercial sample, the surface is corroded in a proportion of over 90%, it is heterogeneous, showing at least three distinct regions; the surface is grooved with irregular shallow channels which delimitate continuous dark portions and is dotted about with small prominent and bright islands (Figure 3, (a) and (b)).

In the case of the casting sample, the entire surface is covered with irregular deep ditches. Very small bright stoppers are randomly buried in these ditches (Figure 3 (c) and (d)).

In order to better understand the qualitative composition of the corroded surface, the EDX line scans were taken at cross sections of surfaces containing different zones. The EDX line scan along lines A-B and B-C of figure 3, shown in figure 4, indicate an enhanced Chromium signal and a decreased Cobalt signal at positions of bright regions, both for commercial and casting samples.



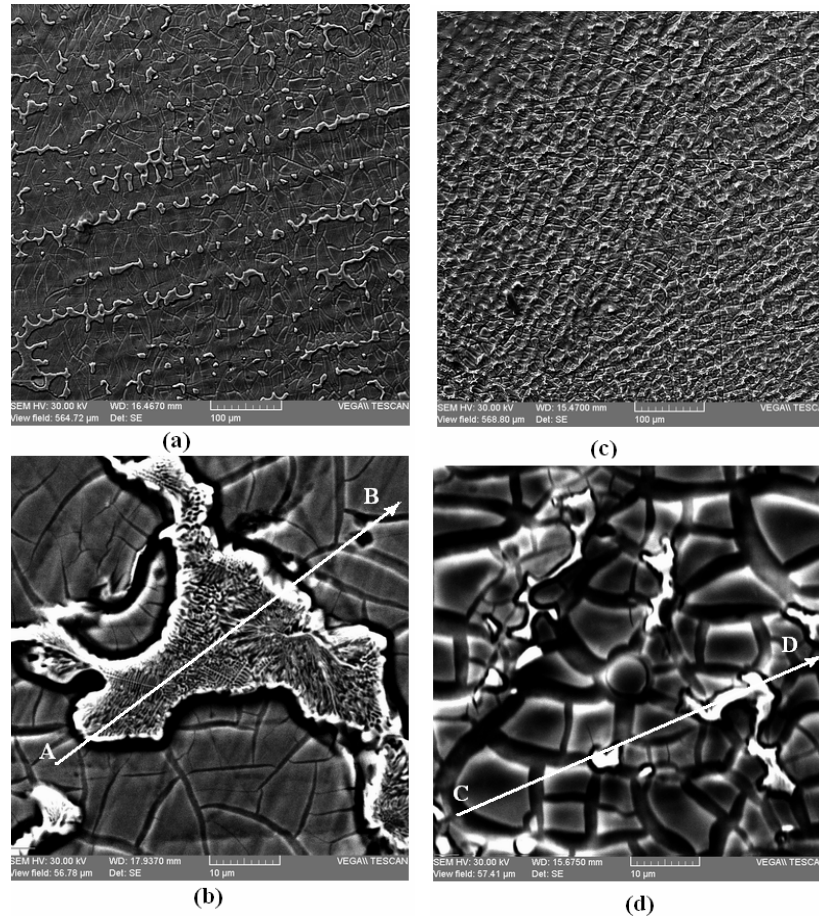


**Fig. 3.** SEM micrographs for CH alloy electrochemically corroded in Afnor saliva by five successive cyclic polarization processes between 0 and 1500 mV; a)- non-casting sample (500 x), (b) – non-casting sample (5000x) (c)- as-cast sample (500x), (d) - as-cast sample (5000x)

These spectra indicate the fact that the Cobalt dissolution during the repeated cyclic polarization treatment takes place only from limited portions of the alloy surface, most probable at the interdendritic regions along with large amounts of precipitate. The

dark portions are most probable chromium oxide, responsible for good resistance to corrosion of this alloy in Afnor saliva. Similar structural modifications for a co-Cr-Mo biomaterial also were reported by Giacomelli et al. [11].

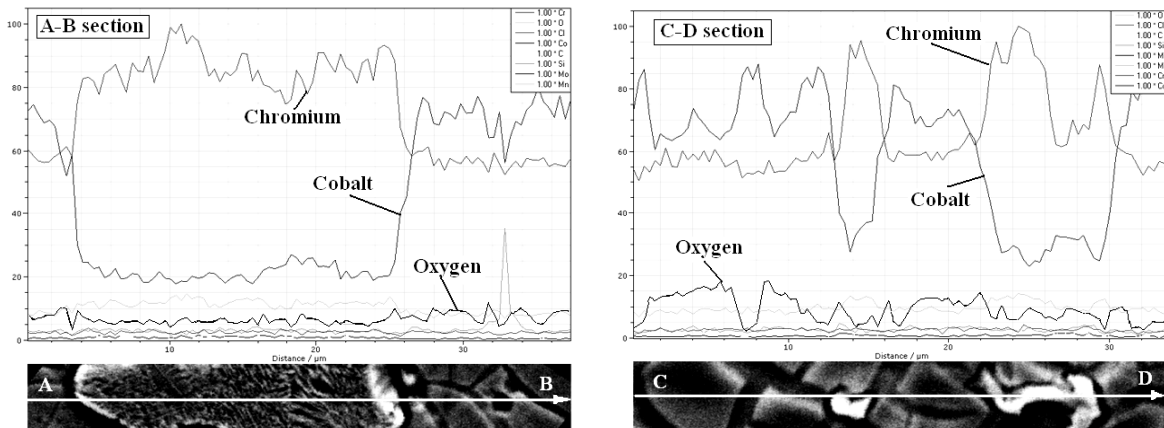


**Fig. 4.** EDX line scan along lines A-B and C-D of figure 3



#### 4. Conclusions

The influence of the casting process on microstructure and corrosion behaviour of a Co-Cr-Mo alloy was studied by linear and cyclic polarization method, Scanning Electron Microscopy and EDX analysis. These studies reveal that in natural aerated Afnor S90-701 artificial saliva, the studied alloy behaves as a corrosion resistant material. In linear and cyclic polarization studies this alloy showed a passive behaviour with a large potential independent region up to a potential of about 500 mV (SCE), followed by a region with significant increase in current density.

By casting, this alloy undergoes a significantly modifications of both internal microstructure and corrosion resistance. At over-potentials greater than 500 mV (SCE) in Afnor saliva this alloy exhibits a generalized corrosion, the surface morphology being dissimilar for commercial and as-cast samples. EDX studies point out that corrosion takes place especially by cobalt dissolution.

#### References

- [1]. **Wulfes H.**, *Precision milling and partial denture constructions*, Bremen: Academia Dental; 2003. p. 259–60; 115–9; 108–13.
- [2]. **Wataha J. C.**, *Alloys for prosthodontic restorations*, J Prosthet Dent. 87, 2002, p. 351–63.
- [3]. **Dong H., Nagamatsu Y., Chen K. K., Tajima K., Kakigawa H., Shi S.**, *Corrosion behavior of dental alloys in various types of electrolyzed water*, Dent Mater J, 22 2003, p. 482–93.
- [4]. **Luthy H., Marinello C. P., Reclaru L., Sharer P.**, *Corrosion considerations in the brazing repair of cobalt based partial dentures*, J Prosthet Dent, 75, 1996, p. 515–24.
- [5]. **German R.**, *The role of microstructure in the tarnish of low-gold alloys*, Metallurgy, 14, 1981, p. 253-266.
- [6]. **Hero H., Jorgensen R.**, *Tarnishing of low/gold dental alloy in different structural states*, J. Dent. Res., 63, 3, 1983, p. 371-376.
- [7]. **Venugopalan R., Gaydon J.**, *A review of corrosion behaviour of surgical implant alloys*. Dept. of Biomedical Engineering, University of Alabama at Birmingham, Technical Review Note, Princeton Applied Research, USA, 2001.
- [8]. **Strandman E.**, *Influence of different types of acetylene-oxygen flames on the carbon content of a dental Co-Cr alloy*, Odontol Revy, 28, 3, 1976, p. 223-238.
- [9]. **Oliveira Bauer J. S., Loguericio A. D., Reis A., Filho L. E. R.**, *Microhardness of Ni-Cr alloys under different casting conditions*, Braz Oral Res, 20, 1, 2006, p. 40-46.
- [10]. **Bane M.**, *Analiza structurii materialelor metalice (The analysis of the structure of metallic materials)*, Editura Tehnică, Bucharest, 1991, p. 184.
- [11]. **Giacomelli F. C., Giacomelli C., Spinelly A.**, *Behaviour of a Co-Cr-Mo Biomaterial in simulated body fluid solutions studied by electrochemical and surface analysis techniques*, J. Braz. Chem. Soc., 15, 4, 2004, p. 541-547.